doi:10.1111/j.1558-5646.2012.01786.x

DIVERSITY-DEPENDENT CLADOGENESIS AND TRAIT EVOLUTION IN THE ADAPTIVE RADIATION OF THE AUKS (AVES: ALCIDAE)

Jason T. Weir[1,2] and Sara Mursleen[1]

[1]*Department of Biological Sciences, University of Toronto Scarborough, Toronto, ON, Canada M1C 1A4*

[2]*E-mail: jason.weir@utoronto.ca*

Received January 18, 2012
Accepted August 6, 2012

Through the course of an adaptive radiation, the evolutionary speed of cladogenesis and ecologically relevant trait evolution are expected to slow as species diversity increases, niches become occupied, and ecological opportunity declines. We develop new likelihood-based models to test diversity-dependent evolution in the auks, one of only a few families of seabirds adapted to underwater "flight," and which exhibit a large variety of bill sizes and shapes. Consistent with the expectations of adaptive radiation, we find both a decline in rates of cladogenesis (a sixfold decline) and bill shape (a 64-fold decline) evolution as diversity increased. Bill shape diverged into two clades at the basal cladogenesis event with one clade possessing mostly long, narrow bills used to forage primarily on fish, and the other with short thick bills used to forage primarily on plankton. Following this initial divergence in bill shape, size, a known correlate of both prey size and maximum diving depth, diverged rapidly within each of these clades. These results suggest that adaptive radiation in foraging traits underwent initial divergence in bill shape to occupy different food resources, followed by size differentiation to subdivide each niche along the depth axis of the water column.

KEY WORDS: Adaptive radiation, Alcidae, auk, cladogenesis, diversity-dependent diversification, ecological opportunity, trait-evolution.

Ecological opportunity, the availability of underutilized niches, is believed to be a key factor driving macroevolutionary divergence during adaptive radiations (Schluter 2000). Ecological opportunity may arise following colonization of a lineage into a newly formed geographic region (e.g., isolated archipelagoes), after a mass extinction, or consequent to the evolution of a "key innovation", enabling exploitation of a resource in novel ways (Schluter 2000; Vamosi and Vamosi 2011). Ecological opportunity is expected to promote rapid divergence of a lineage, which then slows as the number of competing species increases and niche space becomes more densely occupied. This slowdown is predicted to occur both in the rate of cladogenesis (Schluter 2000; Weir 2006; McPeek 2008; Phillimore and Price 2008; Rabosky and Lovette 2008a; Losos 2010) and in the rate of ecologically relevant morphological evolution (Harmon et al. 2003; Agrawal et al. 2009; Losos 2010; Mahler et al. 2011).

Studies utilizing phylogenetic-based methods have generally tested for slowdowns in cladogenesis rate (e.g., Weir 2006; McPeek 2008; Phillimore and Price 2008) or morphological evolution (e.g., Harmon et al. 2010; Kennedy et al. 2012) but rarely both (e.g., Slater et al. 2010; Derryberry et al. 2011; Jønsson et al. in press). Slowdowns in cladogenesis have been inferred from lineage through time plots (which plot the log number of lineages through time) and the associated γ-statistic (which quantifies the severity of slowdowns; Pybus and Harvey 2000) as well as from likelihood-based approaches with time-variable rate parameters (Rabosky and Lovette 2008b). Using these methods, comparative analyses have demonstrated that higher-level taxa often exhibit significant slowdowns in cladogenesis toward the present (Weir 2006; McPeek 2008; Phillimore and Price 2008; Rabosky and Lovette 2008b) with speciose taxa showing the strongest slowdowns (although see Phillimore and Price 2008 for discussion of

EVOLUTION
INTERNATIONAL JOURNAL OF ORGANIC EVOLUTION

biases in this approach). These analyses have relied on models in which cladogenesis rates decline as a function of time. While time may roughly correlate with the decline in ecological opportunity, diversity itself should provide the best correlate. More recently Rabosky and Lovette (2008a) tested models in which the rate of cladogenesis declined as a function of reconstructed diversity rather than time. A constant rate extinction term was added to this model (Etienne et al. 2012), which allowed paleo-diversity levels to be more accurately estimated under nonzero extinction. The diversity-dependent model with extinction term provided a better fit than constant rate models to many clades tested (Etienne et al. 2012), providing strong evidence for one of the predictions of adaptive radiation—that rates of cladogenesis decline as diversity increases and ecological opportunity decreases.

A slowdown in rates of evolution in ecologically relevant traits is the other component of a niche-filling model. Time-dependent models have been developed that allow evolutionary rates to change as a function of time and allow rates at different time points to be estimated directly from the data (Blomberg et al. 2003; Harmon et al. 2010). Harmon et al. (2010) applied these models to a large variety of genera and families (including Darwin's finches and other classic examples of adaptive radiation), and found that time-dependent models fit to body size and body shape were rarely supported over constant rate models. Their results challenge the notion that adaptive radiation often involves a slowdown in evolutionary rates through time. However, time may not always provide a good proxy for clade diversity, especially for clades that exhibited diversification in bursts. A model in which rates of trait evolution declines as a function of diversity rather than time might provide the best fit to such data. Mahler et al. (2011) developed a method correlating magnitude of independent contrasts as a function of time (see also Garland et al. 1992; Richman and Price 1992; Freckleton and Harvey 2006 for earlier implementations of this approach) or as a function of increasing clade diversity. Under a null hypothesis, no correlation of independent contrasts with time or diversity levels is expected. They found that for body length in *Anolis* lizards, clade diversity rather than time best correlated with an observed decline in contrast values toward the present. The independent contrast method provides an elegant means to reject the null hypotheses of constant diversification rates through time. However, Mahler et al. (2011) extended the approach to estimate the magnitude of decline in rates with increasing diversity levels. Quantifying rate declines using independent contrasts is problematic because the contrasts themselves are calculated using a constant rate model (i.e., each contrast assumes a constant rate along the branches connecting the two contrasted daughter lineages to their ancestral node, which for some contrasts can span many millions of years; see Richman and Price 1992). Here, we develop a model with the same objectives—to estimate diversity-dependent rates of trait evolution—but rather than using independent contrasts, we use the likelihood modeling framework developed by Harmon et al. (2010), which uses the underlying phylogenetic covariance matrix. The models we develop allow extinct fossil species to be incorporated into the calculation of diversity-dependent slowdowns in evolutionary rate. We use these models to test for declines in trait evolution in the radiation of the auks (Alcidae).

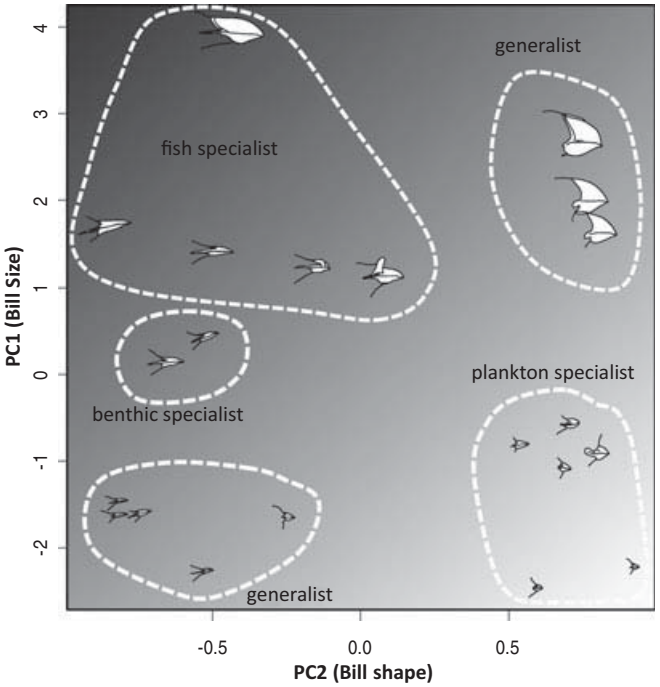

Figure 1. PC1 (bill size) and PC2 (bill shape) for auks. Shading represents degree of diet specialization with dark shading for fish specialization, pale shading for plankton specialization, and intermediate shading for more generalists that feed extensively on both fish and plankton. Bills for each species are drawn on the same scale.

The auks are marine diving birds that represent the northern hemisphere counterpart of the southern hemisphere penguins, both of which have evolved wing structure enabling underwater propulsion to great depths (Nettleship 1996). The modified wing structure in auks and penguins provided a key innovation allowing both groups to use fish, cephalopods, and zooplankton at depths below which most other diving birds can access. Penguins have been recorded to depths of 250 m (Kooyman 1975; Kooyman et al. 1982) and auks to 180 m (Piatt and Nettleship 1985). In contrast, sea ducks, loons, and other diving seabirds have been recorded to maximum depths of only 60 m (Schorger 1947).

Following the evolution of deep diving ability (Piatt and Nettleship 1985), auks radiated into 23 extant and one recently extinct species possessing a spectacular diversity of bill sizes and shapes (Fig. 1). Morphological differences are associated with diet (e.g., Bédard 1969a). The great functional diversity of bills led previous authors to suggest auks represented an adaptive

radiation (Bédard 1969b, 1985). The smallest species—the least auklet (*Aethia pusilla*)—uses its short, wide bill with flattened palatal surface to specialize solely on zooplankton, whereas the largest known species—the recently extinct great auk (*Pinguinus impennis*)—possessed a long, thin bill with reduced palate surface which it used to capture and retain fish (Bédard 1969b). Between these two extremes, most species of auks have varying degrees of specialization to plankton and fish depending on the size and shape of their bill. Here we use a phylogenetic analysis to ask if rates of bill evolution and cladogenesis have each declined as a function of increasing diversity.

Methods

DATED MOLECULAR TREE

A dated molecular tree containing all 23 species of extant auk (including *Brachyramphus perdix*, which is usually considered a subspecies of *B. marmoratus*), as well as the recently extinct great auk (*P. impennis*) was generated from published sequences (Friesen et al. 1996a; Moum et al. 2002; Pereira and Baker 2008) for five mitochondrial (cytochrome b, cytb; NADH dehydrogenase subunit 2, ND2; cytochrome oxidase I, COI; small ribosomal unit 12, 12s; and small ribosomal unit 16, 16s) and one nuclear gene (RAG1)(Genbank accession numbers provided in Table S1). We included a number of outgroups to incorporate external clock calibration events (see Supporting Information). The best supported model of sequence evolution for each gene was previously reported by Pereira and Baker (2008) to be the GTR- Γ-I model. Here, we use the GTR- Γ model because for the correction for invariant sites (I) is already accounted for in the correction among site rate heterogeneity (Γ). For 12s and 16s, we used the GTR- Γ model of sequence evolution. For protein-coding genes, we used the GTR_{112}- Γ_{112} model that allows for separate rates at third codon versus other codon positions. Parameters were estimated separately for each gene. We fixed the ingroup topology to that generated in Figure 2 of Pereira and Baker (2008) (this topology had posterior probabilities greater than 0.98 at all but three nodes) and the outgroup topology to that in Figure 2 of Hackett et al. (2008). BEAST 1.6.1 (Drummond and Rambaut 2007) was used to estimate time-calibrated branch lengths under a relaxed-clock model (with rate variation following a log-normal distribution and Yule speciation prior). We used six internal and five external fossil (minimum age) calibrations, and four external biogeographic (maximum age) calibrations to time-calibrate the tree (Table S2; Fig. S1). We excluded a number of previously used fossil calibrations for Charadriiformes whose affinities have been questioned (see review in Mayr 2011). All calibrations were implemented as uniform distributions with fossil calibrations ranging from 146 Ma (a sufficiently old date) to the age of the calibrating fossil. Uniform distributions for biogeographic-based calibrations ranged from the date of the biogeographic event to 0 Ma (Table S2). Two of our biogeographic calibrations involved the separation of New Zealand from Gondwana ca. 85 Ma (McLoughlin 2001). We used this date as the maximum time period when the endemic New Zealand wrens (suborder Acanthisitti) split off from other passerines and the endemic New Zealand parrots (family Strigopidae) split off from other parrots. Instead, this date is often used as a point calibration (e.g., Ericson et al. 2002; Irestedt et al. 2009; Derryberry et al. 2011), an assumption we consider unjustified, because the ancestor of the clades may have colonized New Zealand any time following continental breakup. Three separate BEAST analyses were run, each for 50 million generations, and trees were sampled every 1000 generations following a 10 million generation burn-in. Median node ages following the burnin were calculated in TreeAnnotator 1.6.1 (Drummond and Rambaut 2007) from the pooled posterior sample of 120,000 trees. We used the time-calibrated phylogeny to estimate rates of cladogenesis and trait evolution.

SLOWDOWN IN LINEAGE DIVERSIFICATION

Using the phylogeny of crown group alcids, we tested for a slowdown in cladogenesis rates (often referred to as speciation rates) towards the present using the γ-statistic (Pybus and Harvey 2000), ρ-statistic (Pigot et al. 2010), and time-dependent and diversity-dependent diversification models. Slowdowns were visualized using LTT plots (lineage through time plost, where the number of reconstructed lineages through time are plotted on a log scale) and are expected to show a downturn if rates of cladogenesis have declined toward the present and background extinction rates are not high (Weir 2006; Rabosky and Lovette 2008b, 2009). For completely sampled clades, this downturn is significant when the γ-statistic has a value less than –1.645 (using a one-tailed test; Pybus and Harvey 2000). The related ρ-statistic compares the net rates of diversification in the first and second half of a phylogenetic tree. Values of zero illustrate no change in rate through time whereas values less than 0 indicate a slowdown in rate to the present (with the most extreme slowdowns having a maximum value of –1). Past authors have occasionally corrected for the lag-time between population splitting and recognition of populations as species by truncating the time period to which unsampled intraspecific level splits are expected to date near the tips of phylogenies (e.g., Weir 2006, Phillimore and Price 2008). We did not truncate our tree because phylogeographic studies conducted on all 10 polytypic auk species uncovered only shallow levels of genetic differentiation and a complete lack of reciprocal monophyly in mitochondrial DNA markers between subspecies (Moen 1991; Friesen et al. 1996b, 2005; Kidd and Frisen 1998; Pearce et al. 2002; Walsh and Friesen 2003; Johnsen et al. 2009; Birt et al. 2012) suggesting we have sampled all phylogenetically recognizable lineages.

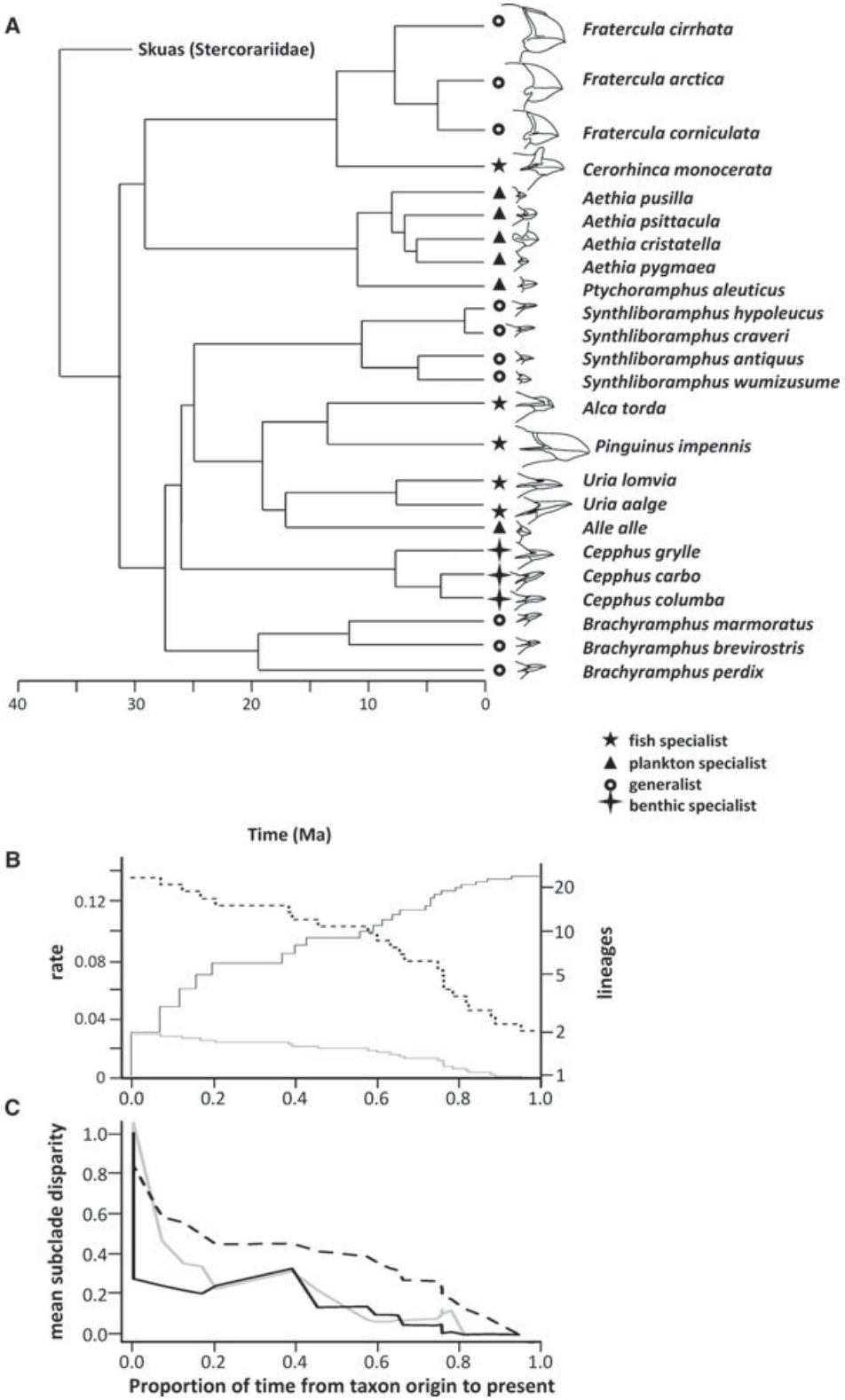

Figure 2. Time-calibrated phylogeny and analyses of diversification and trait evolution in the auks. (A) Time-calibrated phylogeny generated in BEAST. (B) A lineage through time plot (black line) and plots of cladogenesis rate (gray line) and the rate of bill shape evolution (black dotted line) at each time point under the best-fit models in which rates changes linearly as a function of diversity. (C) Mean subclade disparity through time for bill size (PC1, gray) and bill shape (PC2, black). Dashed line indicates expected subclade disparity under a constant rates BM model.

We fit time-dependent diversification models that estimate rates of cladogenesis (λ) and extinction (μ) from our reconstructed phylogeny. These models allow λ and μ to decline linearly or exponentially as a function of time (t) (Rabosky and Lovette 2008a):

$$\begin{aligned} \lambda(t)_{linear} &= xt + \lambda_0 \\ \mu(t)_{linear} &= xt + \mu_0, \end{aligned} \quad (1)$$

$$\begin{aligned} \lambda(t)_{exponential} &= \lambda_0 \exp(-rt), \\ \mu(t)_{exponential} &= \mu_0 \exp(-rt), \end{aligned} \quad (2)$$

where x is the slope of the linear model, and r the rate parameter of the exponential model. We fit four time-dependent models in which cladogenesis changed linearly (TDλ_{lin}) or exponentially (TDλ_{exp}) through time without extinction, or in which both cladogenesis and extinction changed linearly (TDλ_{lin}-TDμ_{lin}) or exponentially (TDλ_{exp}-TDμ_{exp}) through time. These time-dependent models were compared to a constant rate pure birth model (CRλ) and a constant rates birth-death model (CRλ-CRμ).

We also tested both linear and exponential models of diversity-dependent cladogenesis (Nee et al. 1992; Rabosky 2006; Rabosky and Lovette 2008a). Under the diversity-dependent exponential model (DDλ_{exp}), the cladogenesis rate, λ, is a function of the number of lineages (N) (Rabosky and Lovette 2008a):

$$\lambda(N) = \lambda_0 N^{-r}, \quad (3)$$

where λ_0 is the initial cladogenesis rate and r determines the exponential rate of decline ($r < 0$) or increase ($r > 0$) in cladogenesis rates. Under the linear model (DDλ_{lin}) of diversity-dependent cladogenesis (i.e., the logistic model adapted from population biology), the cladogenesis rate slows linearly as N approaches a species-level "carrying capacity", K, which can be interpreted as the maximum number of lineages sustainable at equilibrium (Rabosky and Lovette 2008a):

$$\lambda(N) = \lambda_0 \left(1 - \frac{N}{K}\right). \quad (4)$$

Etienne et al. (2012) added a constant-rate extinction parameter, μ, to the DDλ_{lin} and DDλ_{exp} models (DDλ_{lin}-CRμ and DDλ_{exp}-CRμ) that allow the cladogenesis rate in these diversity-dependent models to change as a function of estimated paleo-diversity levels (after accounting for extinct species), rather than reconstructed paleo-diversity levels (as obtained from phylogenetic trees of extant species with no information about extinct lineages). If extinction is nonzero, the maximum number of species sustainable at equilibrium is $K' = \lambda_0 K/(\lambda_0 - \mu)$.

Likelihood functions (all of which condition on survival of the phylogeny to the present) for these models are presented in Nee et al. (1994), Rabosky and Lovette (2008a), and Etienne et al. (2012). We used the R packages DIVERSITREE (Fitzjohn 2010), LASER (Rabosky 2006), and DDD (Etienne et al. 2012) to obtain the maximum likelihood estimates of parameters for each of the models discussed above. The model best supported by the data was considered to be the one with the lowest Akaike Information Criterion (AIC) and highest Akaike weights.

SLOWDOWN IN MORPHOLOGICAL EVOLUTION

We used the following morphometric measurements for adult males from Bédard (1969b) for all species of auks (except *Synthliboramphus wumizusume*, *B. perdix*, and *Cepphus carbo* for which data were not available): bill length (exposed culmen), bill depth (maximum depth), bill width (at posterior edge of nostrils), and gape (measurements provided in Supporting Information). Bill depth for the great auk (*P. impennis*) was obtained from Gaston and Jones (1998). We performed a principal component (PC hereafter) analysis based on the covariance matrix on log-transformed mean measurements for each species. We used the first two PCs in our analysis of rates of morphological evolution through time. Because mean values for most measurements were based on sample sizes of tens to hundreds of individuals, we ignore measurement error.

We tested six models of morphological evolution: (1) a constant rates Brownian motion model (BM hereafter) with a single rate parameter β, (2) an Ornstein–Ulhenbeck model (OU) in which β is held constant through time, but evolutionary divergence is constrained around an optimal value (Hansen 1997; Butler and King 2004; Harmon et al. 2010), (3) a time-dependent linear model (TDβ_{lin}) in which β changes linearly through time (t) from the root to the tips: $\beta(t) = \beta_0 + bt$ where β_0 is the initial rate parameter and b is the slope (Supporting Information in Harmon et al. 2010), (4) a time-dependent exponential model (TDβ_{exp}; also referred to as the "early-burst" model, Harmon et al. 2010) in which β changes exponentially through time: $\beta(t) = \beta_0 e^{(at)}$ where a is a parameter describing change through time (Blomberg et al. 2003; Harmon et al. 2010), (5) a diversity-dependent linear model (DDβ_{lin}) developed here in which β changes linearly with changing species diversity in a clade (n): $\beta(n) = \beta_0 + bn$, and (6) a diversity-dependent exponential model (DDβ_{exp}) developed here in which β changes exponentially with changing species diversity in a clade: $\beta(t) = \beta_0 e^{(at)}$. The likelihood function of these models is (Harmon et al. 2010)

$$L = \frac{exp\{-1/2[\mathbf{X} - \mathbf{E}]'(\mathbf{V})^{-1}[\mathbf{X} - \mathbf{E}]\}}{(2\pi)^N \times \det(\mathbf{V})}, \quad (5)$$

where $\mathbf{X}$ is the vector of phenotypes, $\mathbf{E}$ is the covariance matrix of expected tip values and follows a multivariate normal distribution, and $\mathbf{V}$ is the expected covariance matrix under each model of evolution. $\mathbf{V}$ has elements V_{ij} determined by the phylogeny and scaled according to the evolutionary model (eqs. 6–9 from

Harmon et al. 2010; eqs. 10 and 11 developed here):

$$V_{ij(\mathbf{BM})} = \beta S_{ij}, \tag{6}$$

$$V_{ij(\mathbf{OU})} = \frac{\beta}{2\alpha} e^{-2\alpha(T_M - S_{ij})}(1 - e^{-2\alpha S_{ij}}), \tag{7}$$

$$V_{ij(\mathrm{TD}\beta_{lin})} = \beta_0 S_{ij} + \frac{b S_{ij}^2}{2}, \tag{8}$$

$$V_{ij(\mathrm{TD}\beta_{exp})} = \beta_0 \left(\frac{e^{r S_{ij}} - 1}{r} \right), \tag{9}$$

$$V_{ij(\mathrm{DD}\beta_{lin})} = \sum_{m=2}^{M} (\beta_0 + b n_{m-1})(\max(S_{ij} - T_{m-1}, 0) - \max(S_{ij} - T_m, 0)), \tag{10}$$

$$V_{ij(\mathrm{DD}\beta_{exp})} = \sum_{m=2}^{M} (\beta_0 \times \mathrm{e}^{r n_{m-1}})(\max(S_{ij} - T_{m-1}, 0) - \max(S_{ij} - T_m, 0)), \tag{11}$$

where S_{ij} represents the shared path length from the root of the phylogeny to the common ancestor of species i and j, b and r are parameters describing the change of rate under linear and exponential models, respectively, α is the constraint parameter of the OU model, and N is the total number of species on the phylogenetic tree. M is two plus the number of points on a tree at which species richness increases (due to cladogenesis) or decreases (due to extinction; see below for adding extinct species), $\boldsymbol{n}$ is a vector of length $M - 1$ providing the number of species occuring during each internode interval (with the interval from the youngest node to the tips included). Here, we assume that $n = 2$ at the basal node of the reconstructed phylogeny, an assumption that will not be true if extinct stem groups overlapped temporally with the lineages representing the basal node. T_1 is 0, T_2:T_{M-1} are the times from the basal node of the phylogeny to each successive node, and T_M is the time from the basal node to the tips. Models in equations (7)–(11) involve rescaling the original phylogenetic variance covariance matrix, an approach that goes back to Pagel (1994).

The diversity-dependent models define a separate rate to every internode interval on a phylogeny so that rates change linearly ($\mathrm{DD}\beta_{\mathrm{lin}}$) or exponentially ($\mathrm{DD}\beta_{\mathrm{exp}}$) as a function of n. These models can incorporate extinct species to provide a better estimate of paleo-diversity levels (n) at each internode interval. To include a fossil species, a node is added to any of the lineages on the tree at the time point when the fossil species originated. The branch descending from that node represented by the fossil species is truncated at the point in time when the fossil species went extinct. Every fossil species added to a tree increases the value of M by a factor of two. Also, if trait values are lacking for an extant species on a phylogeny, these can be added to paleo-diversity estimates (n) when fitting the models in equations (10) and (11) provided the ages at which species with missing trait data join the tree are known. For both extinct species or missing extant species added to a tree, S_{ij} is calculated only for extant species with trait data. We lacked measurements for three extant species (*S. wumizusume*, *B. perdix*, and *C. carbo*) but because we know the node ages at which they join the tree, we were able to incorporate them into our paleo-diversity estimates. Although extinct fossil auk species are known to occur, we excluded these from our paleo-diversity estimates because the fossil record for auks is poorly represented prior to the late Miocene. Our estimates of paleo-diversity through time are estimated only from the reconstructed phylogenetic tree, with extinct fossil species excluded.

For PC1 and PC2, we compared the likelihoods of each model using AIC and Akaike weights. As a second approach for PC2, we used Phylogenetic Monte Carlo (PMC hereafter) power analyses (Boettiger et al. 2012). PMC performs pairwise comparisons between models (models A and B, where A is the "null" model and B is the "test" model) using three steps. (1) Maximum likelihood estimates of parameters were obtained for models A and B and the likelihood ratio was calculated [δ = –2 × (likelihood A/likelihood B)]. (2) These parameter estimates were used to simulate trait data 2000 times under each model ($\mathrm{A_{sim}}$, $\mathrm{B_{sim}}$). (3) Both models were refit to each simulated dataset ($\mathrm{AA_{sim}}$, $\mathrm{BA_{sim}}$ $\mathrm{AB_{sim}}$, $\mathrm{BB_{sim}}$ where $\mathrm{AA_{sim}}$ is the likelihood fit of model A to $\mathrm{A_{sim}}$) and two likelihood ratios were calculated for each simulation,

$$\delta_{\mathrm{A}} = -2 \times \ln(\mathrm{likelihoodAA_{sim}}/\mathrm{likelihoodBA_{sim}}),$$

$$\delta_{\mathrm{B}} = -2 \times \ln(\mathrm{likelihoodAB_{sim}}/\mathrm{likelihoodBB_{sim}}).$$

The probability of rejecting model A (the null) relative to model B (the test) is simply the proportion of simulated $\delta_{\mathrm{A}} > \delta$. The statistical power of the test (the probability that we correctly reject model A when the data came from model B) is calculated with a false-positive rate of 5% and is the proportion of simulated δ_{B} > the 95th percentile of the simulated distribution of δ_{A} (for further details see Boettiger et al. 2012). The PMC method was coded into R and is available upon request.

SUBCLADE DISPARITY

Under adaptive radiation, clades are expected to diversify rapidly into different regions of niche space early in the radiation (e.g., Ciampaglio et al. 2001; Harmon et al. 2003). We test this by looking at mean subclade disparity in PC1 and PC2 through time across the auk phylogeny. Expected mean subclade disparity through time under a best-fit BM was calculated using the "ddt.full" function in the R package GEIGER (Harmon et al. 2008). Lower than expected actual mean subclade disparity values

Table 1. Support for different models of diversification fit to the phylogeny of auks. ΔAIC scores (AIC—AIC score for best-fit model) shown for all models. Calculation of Akaike weights exclude CRλ-CRμ and TDλ$_{exp}$-TDμ$_{exp}$, because the extinction term in these models was estimated to be zero and they are equivalent to the simpler CRλ and TDλ$_{exp}$ models, respectively. λ and μ are the birth and death rates, respectively, for constant rates (CR) models. For the variable rates models (DD and TD), λ and μ represent the initial birth and death rates, respectively, at the basal node of the tree (for diversity-dependent models at $n = 2$). λ-par and μ-par refer to the parameters that describe how λ and μ, respectively, change either as a function of time or as a function of diversity. Values in bold show the best-fit model.

Model	λ	λ-par	μ	μ-par	loglike	n	ΔAIC	Akaike weights
CRλ	0.0636				−31.005	1	2.512	0.096
CRλ-CRμ	0.0636		0.0000		−31.114	2	4.512	–
TDλ$_{lin}$	0.0330	$x = -0.0033$			−29.626	2	1.754	0.140
TDλ$_{lin}$-TDμ$_{lin}$	0.0299	$x = -0.0299$	0.0400	$x = -0.031$	−30.832	4	8.166	0.006
TDλ$_{exp}$	0.0409	$r = -0.0382$			−29.864	2	2.230	0.111
TDλ$_{exp}$-TDμ$_{exp}$	0.0409	$r = -0.0382$	0.0007	$r = 0.000$	−29.864	4	6.230	0.015
DDλ$_{lin}$	0.1358	$K = 28.89$			−28.749	2	**0.000**	**0.338**
DDλ$_{lin}$-CRμ	0.1355	$K = 28.91$	0.0000		−28.749	3	2.000	–
DDλ$_{exp}$	0.3047	$r = 0.6329$			−29.195	2	0.893	0.216
DDλ$_{exp}$-CRμ	0.4555	$r = 467.1$	0.0047		−29.210	3	2.922	0.078

indicate larger than expected differences and little overlap in morphometric space between subclades as expected under adaptive radiation. Larger values of mean subclade disparity indicate extensive overlap between subclades in morphometric space. These predictions for low subclade disparity under adaptive radiation are complementary to, but not identical with, our predictions that rates of trait evolution should decline through time. Declining rates of trait evolution need not necessarily result in reduced subclade disparity. Thus together, they provide for a more powerful test of adaptive radiation than either does individually. To determine if observed and expected values of mean subclade disparity differed significantly, we calculated the morphological disparity index (MDI)—the overall difference between the expected and observed average disparity across the tree (Harmon et al. 2003). Significance was determined by calculating MDI for 1000 simulations under Brownian motion along the phylogeny. A significantly negative value for MDI indicates that mean subclade disparity is lower than expected under Brownian motion, as expected if ecological opportunity has resulted in subclade specialization in different regions of niche space.

Results

DATED MOLECULAR TREE

The dated phylogeny (Fig. S1) suggests that the lineage leading to crown group auks split from its sister lineage, the Stercorariidae, at approximately 36.6 Ma (Fig. 2A), slightly before the oldest known auk fossil (dated at 36–34.2 Ma) that can unambiguously be assigned to the auks (Chandler and Parmley 2002; Mayr 2009 p. 87, 2011; Smith 2011). Others have calibrated the origin of auks as much older (~65 Ma in Pereira and Baker 2008). The younger date that we obtained resulted mostly from rejection of several fossils as being suitable for calibration (Mayr 2011).

Our dating suggests the crown group of auks began diversifying at 31.5 Ma, shortly after they diverged from the clade leading to the Stercorariidae. The youngest sister species pair of Alcids (*S. craveri* and *S. hypoleucus*) is dated at ca. 1.7 Ma. The calibrated tree also suggests that penguins and Procellariformes last shared a common ancestor at 78 Ma, 17 Ma before the oldest known fossil penguin. The lineage leading to New Zealand wrens colonized New Zealand at ca. 68 Ma (Brown and Van Tuinen 2011 obtained a similar date) whereas the lineage leading to the New Zealand parrots (family Strigopidae) diverged from other parrots at ca. 53 Ma. These dates are 17–32 Ma older than the date when New Zealand broke away from Gondwana. The discrepancy suggests that the age of New Zealand should not be used as a point calibration as often employed, but rather as a maximum age calibration as implemented here.

SLOWDOWN IN LINEAGE DIVERSIFICATION

The LTT plot (Fig. 2B) exhibited a strong downturn, a result mirrored by a strongly negative value of the ρ-statistic ($\rho = -0.62$) and a significantly negative value of the γ-statistic ($\gamma = -1.73$, $P = 0.042$). The best supported model of diversification was DDλ$_{lin}$ in which rates declined linearly as a function of N (Akaike weight = 0.34; Table 1; Fig. 2B). Under this model, carrying capacity K was estimated to be ca. 29 species, five species higher than the current level of auk diversity (24 species). The next best supported model was DDλ$_{exp}$ (Akaike weight = 0.22). Together, diversity-dependent models received Akaike weights of 0.63, time-dependent models received weights of 0.27, and

Table 2. Support for different models of trait evolution fit to the first two principal components (PC1 and PC2) of bill measures for the auks. For each PC, the model with the lowest ΔAIC score (AIC—AIC score for best-fit model) (bold) and highest Akaike weights is considered to best fit the data. Calculation of Akaike weights exclude OU for both PC1 and PC2, because the term α was estimated to be zero and thus is equivalent to the simpler BM model. β is the evolutionary rate parameter for constant rates (CR) models. For variable rates models (DD and TD), β represents the evolutionary rate at the basal node in the phylogeny. par refers to the parameter that describes how β changes (b = slope for linear models, r = parameter of the exponential models, α = bounding parameter under the OU model). Values in brackets for PC2 are the median parameter values reestimated from 2000 datasets simulated along the auk phylogeny (with each simulation using the maximum likelihood parameter estimates for each model).

	β	par	loglike	n	ΔAIC	Akaike weights
PC1 (bill size)						
BM	0.0947		−34.724	1	**0.000**	**0.275**
OU	0.0947	$\alpha = 0.0000$	−34.724	2	2.000	–
$TD\beta_{lin}$	0.3329	$b = -0.0100$	−34.085	2	0.722	0.192
$TD\beta_{exp}$	0.2540	$r = -0.0460$	−34.368	2	1.288	0.145
$DD\beta_{lin}$	0.2193	$b = -0.0082$	−34.008	2	0.554	0.209
$DD\beta_{exp}$	0.2300	$r = -0.0659$	−34.152	2	0.856	0.179
PC2 (bill shape)						
BM	0.0093		−10.309	1	3.880	0.071
	(0.0876)					
OU	0.0093	$\alpha = 0$	−10.309	2	5.880	–
$TD\beta_{lin}$	0.0360	$b = -0.00114$	−8.091	2	1.444	0.241
	(0.02731)	(−0.00087)				
$TD\beta_{exp}$	0.0382	$r = -0.06830$	−9.446	2	4.154	0.062
	(0.03207)	(0.1124)				
$DD\beta_{lin}$	0.0303	$b = -0.00136$|	−7.369	2	**0.000**	**0.495**
	(0.0243)	(−0.00109)				
$DD\beta_{exp}$	0.0458	$r = -0.1262$	−8.698	2	2.658	0.131
	(0.1613)	(−0.0477)				

constant rate models received weights of 0.10. These results best support diversity-dependent cladogenesis in the auks. The $DD\lambda_{lin}$-CRμ model did not result in an improved fit to the data over $DD\lambda_{lin}$ and estimated extinction rates to be near zero (Table 1).

SLOWDOWN IN MORPHOLOGICAL EVOLUTION

The first two PCs (Fig. 1) together accounted for 96% of the variance (PC1 83%, PC2 13%). PC1 had positive (and approximately equal) loadings for all four measurements and represents a bill size component. PC2 had positive loadings for bill depth (0.46) and width (0.49), and negative loadings for bill length (–0.31) and gape (–0.67). PC2 represents a bill shape component, with more positive values indicating short, but thick and wide, bills, and more negative values indicating long, thin, and narrow bills.

For PC1, AIC and Akaike weights best supported the BM model (Table 2). The next best supported model was the diversity-dependent linear ($DD\beta_{lin}$) model, although this model had only slightly higher support than other diversity- or time-dependent models. For PC2, AIC and Akaike weights best supported the $DD\beta_{lin}$ model that received twice as much support than the next best-fit model, the time-dependent linear ($TD\beta_{lin}$) model; and almost four times more support than the third best-fit model, the diversity-dependent exponential ($DD\beta_{exp}$) model (Table 2; Fig. 2B). Akaike weights indicate these three models together received more than six times more support than all other models (Table 2).

We did not implement the PMC method for PC1 given the lack of support in AIC values for more complex models over the BM model. For PC2, we compared BM, $DD\beta_{exp}$, and $TD\beta_{exp}$ to our two models with highest AIC support, $DD\beta_{lin}$ and $TD\beta_{lin}$. We also compared $DD\beta_{lin}$ to $TD\beta_{lin}$ and $TD\beta_{lin}$ to $DD\beta_{lin}$. We did not include the OU model in PMC comparisons given the bounding parameter of this model was estimated to be 0, thus reverting to the nested BM model. Results for the PMC method closely mirrored those for AIC (Table 3). For the $DD\beta_{lin}$ model, AIC was strongly correlated with both the probability of rejecting each of the models contrasted with $DD\beta_{lin}$ ($r = -0.94$) and with the statistical power to discriminate between contrasted models ($r = 0.79$). BM and $TD\beta_{exp}$ were each rejected when compared to either $TD\beta_{lin}$ or $DD\beta_{lin}$ with moderate to high statistical power (Table 3). Tests comparing $DD\beta_{exp}$ to either $TD\beta_{lin}$ or $DD\beta_{lin}$ were close to, but not quite significant. PCM was unable to differentiate between $TD\beta_{lin}$ and $DD\beta_{lin}$ with both models receiving similar

Table 3. Phylogenetic Monte Carlo (PMC) tests showing the probability of rejecting the "null" model in favor of either $TD\beta_{lin}$ or $DD\beta_{lin}$ for PC2. The statistical power of each test to reject the null when the simulated data are produced using either $TD\beta_{lin}$ or $DD\beta_{lin}$ is shown in brackets. Contrasted models are sorted by ΔAIC in descending order.

Null Model	ΔAIC	$TD\beta_{lin}$	$DD\beta_{lin}$
$TD\beta_{exp}$	4.15	0.014 (0.169)	0.034 (0.39)
BM	3.88	0.017 (0.59)	0.014 (0.72)
$DD\beta_{exp}$	2.66	0.062 (0.094)	0.0725 (0.21)
$TD\beta_{lin}$	1.44	–	0.208 (0.12)
$DD\beta_{lin}$	0	0.602 (0.096)	–

support and low power to discriminate between them (Table 3). In contrast to most other models, both $TD\beta_{lin}$ and $DD\beta_{lin}$ performed well at correctly reestimating model parameters from simulated data along our phylogeny (Table 2).

Average subclade disparity (Fig. 2C) for PC1 did not decline below the Brownian motion expectation until the second node in the phylogeny and thereafter remained lower than expected. In contrast, average subclade disparity dropped sharply at the first node for PC2 and remained low thereafter. The MDI statistic was significantly negative for PC2 ($P = 0.046$), but not for PC1 ($P = 0.144$).

Discussion

The auks have long been considered a separate suborder of their own (Alcae) within the shorebirds (Charadriiformes), due to their peculiar morphology associating with diving (Nettleship 1996). However, recent phylogenetic results suggest they evolved from gull-like ancestors and should be placed within the suborder Lari (Figs. 2, S1; Paton et al. 2003; Paton and Baker 2006; Baker et al. 2007; Pereira and Baker 2008; Mayr 2011), a group that includes the gulls, terns, skimmers, skuas, and coursers; and which, with the exception of the auks, are incapable of diving (although some groups plunge for fish just below the water's surface). Our phylogeny dates the crown group of auks at 31.5 Ma, only five million years after the divergence of auks from their sister family—the skuas (Stercorariidae)—a species poor group (five to seven species) with a highly conserved gull-like morphology. The implication is that the highly modified diving morphology of auks evolved rapidly within a relatively narrow time window. The subsequent diversification of auks supports two key expectations of a niche-filling model of adaptive radiation—diversity-dependent cladogenesis and diversity-dependent evolution of traits important for resource utilization. We discuss both of these here in turn and consider the effect of extinction on these results.

Diversity-Dependent Cladogenesis

A downturn in LTT plots and negative γ- and ρ-statistics point to a net decline in cladogenesis rates toward the present in the auks (Fig. 2B), and many other higher-level taxa (Weir 2006; McPeek 2008; Phillimore and Price 2008; Jønsson et al. in press; but see Slater et al. 2010 and Derryberry et al. 2011). This decline for auks was best fit by a diversity-dependent model in which rates of cladogenesis declined as a function of increasing, within-clade diversity levels. Recent application of diversity-dependent models suggest they often outperform time-dependent models (Rabosky and Lovette 2008a; Etienne et al. 2012; Jønsson et al. in press), although support for a diversity-dependent over time-dependent model in the auks was moderate. Under the best-fit diversity-dependent model ($DD\lambda_{lin}$), cladogenesis rates in auks declined sixfold from initial reconstructed diversity levels at the root of the tree ($n = 2$) to the present ($n = 24$).

The $DD\lambda_{lin}$ model estimated the species carrying capacity (K) to be close to 29, implying that the radiation of auks, currently at 24 extant species, is approaching this capacity, and that only moderate increases in future diversity can be expected. Although the fossil record of auks is not well understood, the early Pliocene fossil records indicate auk diversity may have exceeded this estimated carrying capacity, suggesting either that the number of auk species overshot their ecological equilibrium before declining in the late Pliocene, or that estimates of the carrying capacity obtained from our phylogeny do not accurately reflect past ecological dynamics.

Diversity-dependent cladogenesis may arise for several reasons (Rabosky and Lovette 2008a; Rabosky and Lovette 2009). The usual ecological explanation is that niche space at the local community scale becomes progressively occupied during the course of an adaptive radiation. When local communities are densely packed with competitors, it may be more difficult for newly formed allopatric species to invade these communities. Thus, through the course of an adaptive radiation, we expect new species diverging in allopatry (the primary geographic mode of speciation in birds; Coyne and Price 2000; Coyne and Orr 2004; Phillimore et al. 2008) to experience increased difficulty in achieving geographic sympatry with each other as diversity levels in local communities accumulates. Following the initial evolution of a key adaptation allowing entry into a new adaptive zone, opportunities for allopatric speciation will be high as a clade expands into new geographic regions lacking competitors. Initially sympatry is achieved easily, allowing for frequent range expansions, and renewed rounds of allopatric speciation. As local ecological communities become saturated and sympatry becomes more difficult to achieve (i.e., sympatry in terrestrial birds is currently estimated to require on average 1.7 million years at high latitudes and 3.2 million years at the equator; Weir and Price 2011) range

expansions and further rounds of allopatric speciation become less frequent and diversification rates slow (Phillimore and Price 2008, 2009; Weir and Price 2011; see also Pigot et al. 2010 who showed that stable geographic ranges with limited capacity for range expansions also result in a diversity-dependent signature). Thus, we expect that niche filling and the resulting decline in ecological opportunity at local community scales reduces opportunity for allopatric speciation over broader geographic scales, resulting in a clade-wide pattern of diversity-dependent cladogenesis.

Diversity-Dependent Trait Evolution

Both PC1 and PC2 (Fig. 1) appear to be ecologically relevant traits as they correlate with diet in auks. Plankton specialists have small bills (negative values for PC1) with a short, thick, and wide shape (positive values for PC2). Fish specialists have large bills (positive values for PC1) with a long, narrow shape (negative values for PC2). Between these extremes, species with small, but long and narrow bills (the murrlets and guillemots: *Cepphus*, *Synthliboramphus*, *Brachyramphus*), or large, but short and thick bills (the puffins, *Fratercula* and *Cerorhinca*), are both generalists, feeding extensively on fish and plankton.

Here, we develop diversity-dependent models of trait evolution that allow us to test whether rates of evolution in ecologically relevant traits decline as a function of increasing diversity within a clade. Our diversity-dependent linear model provided the best fit for bill shape (PC2) whereas a constant rates BM best-fit bill size (PC1). This mixed support for the diversity-dependent model suggests that bill shape may have been more susceptible than bill size to declining ecological opportunity during the radiation of auks. Bill size is not only an indicator of diet specialization, but is also strongly correlated with body mass ($r = 0.92$), and body mass is associated with diving depth, with larger species capable of diving to deeper depths than smaller species (Piatt and Nettleship 1985). Because bill size is relevant to multiple ecological axes in auks, opportunity for its evolution may continue even after opportunity in one or more of its ecological axes has declined.

Our data also suggest that bill shape began diversifying into distinct subclades before bill size. Plots of mean subclade disparity through time (Fig. 2C) indicate a sharp initial decline in disparity of bill shape at the basal node in the auks. This resulted in one clade possessing mostly short, thick, and wide bills; the other, mostly long, thin, and narrow bills (Fig. 2A). Subclade disparity in bill shape remained low throughout the remainder of the radiation suggesting that subclades overlap little in bill shape. In contrast, subclade disparity in bill size dropped below its Brownian motion expectation at the second node in the phylogeny, and remained low thereafter (Fig. 2C). These results suggest that shape was the initial axis of variation along which the bills of auks diversified. This was followed shortly after by bill size. We suggest that auks initially diversified into a plankton-specializing clade (short, wide bills) and a fish-specializing clade (long, thin bills) associated primarily with bill shape, and that subsequent size evolution (both bill size and its correlate, body mass) allowed species in each clade to specialize on different size categories of prey and different depths in the water column.

Richman and Price (1992) found that *Phylloscopus* warblers in the Himalayas diversified first along an axis of bill size (thought to be a correlate of diet in this group), and then along an axis of elevation/habitat within each size category. The evolution of elevational differences following diet specialization in *Phylloscopus* mirrors the proposed evolution of differences in diving depths following diet specialization in auks. Results for auks and *Phylloscopus* challenges the habitat-first rule (Diamond 1986) where divergence in habitat is thought to be followed by diet divergence in adaptive radiations (see critiques in Schluter 2000 ch. 3; Price 2008, ch. 5; Glor 2010). Subclade disparity for the vangas of Madagascar, however, exhibited a more complicated pattern. Like the auks and *Phylloscopus*, vanga subclades differentiated early in their radiation into different size categories. However, unlike the auks, vangas retained higher than expected subclade disparity in bill shape through most of their radiation (Jønsson et al. in press), suggesting that selective pressure to diversify in bill shape did not decline with increasing diversity as expected under a simple model of adaptive radiation. The authors interpreted this result as evidence for a series of nested adaptive radiations occurring within vanga subclades at different points in time, the combined effect of which maintained higher than expected subclade disparity in bill shape. Together, these studies suggest that some aspects of adaptive radiations may often proceed in predictable sequences (with initial evolution into broadly different foraging niches, followed by subsequent spatial partitioning within each niche) as ecological opportunity declines, but suggest that these patterns may become difficult to disentangle for groups (e.g., vangas) entering new adaptive zones at multiple time points in their evolutionary history.

In contrast to our findings for auks, a recent comparative analysis failed to find strong support for declines in evolutionary rate of body size and shape across a wide variety of genera and other higher level taxonomic groups, including some classic examples of adaptive radiation (Harmon et al. 2010). The authors concluded that slowdowns in rates of trait evolution may not be a common component of adaptive radiation as generally believed. One group they analyzed, which failed to support declining rates of evolution, was the auks. Here we used only a subset of measurements used by Harmon et al. (2010) for the auks—those of the bill—and found strong support for a linear decline in rates of evolution in bill shape (but not size) with either increasing diversity (best fit) or time (second best fit). One possibility for the discrepancy in these findings is that we restricted our measurements to

just the bill, a feature that is directly related to diet specialization. By including measurements of other body parts (i.e., tarsus, wing, claw, tail, etc.), it is possible that the key PCs recovered by Harmon et al. (2010) for auks did not strongly reflect ecologically relevant variation to diversity-dependent changes in evolutionary rate. The Harmon et al. study also lacked measurements for the largest species, the greak auk (*P. impennis*) that we included here. Another possibility is that the time-dependent model of trait evolution used in the Harmon et al. (2010) study (one in which rates change exponentially through time; $TD\beta_{ex}$) performs poorly compared to the diversity-dependent model developed here.

Our results for PC2 in auks did reject the $TD\beta_{exp}$ model (i.e., also known as the early burst model), but were unable to reject a model in which rates changed linearly through time ($TD\beta_{lin}$). Time-dependent models should give similar results to diversity-dependent models when diversity increased steadily with time (in which case time can be used as a proxy for diversity). However, time-dependent models would be expected to perform poorly for phylogenetic trees that experienced bursts of cladogenesis and/or extinction, because time would be expected to correlate poorly with diversity estimates in such cases. While the improved fit of a diversity-dependent model over a time-dependent model in PC2 for auks was moderate, our results nevertheless do suggest that diversity-dependent models should be routinely considered, especially for phylogenies that exhibit bursts of diversification. The diversity-dependent models we develop here may prove most useful for groups with a well-documented fossil record, where paleo-diversity levels can include extinct fossil species.

Extinction and Diversity-Dependent Evolution

Of the diversity-dependent diversification models we tested that included an extinction term, the best-fit model ($DD\lambda_{lin}$-$CR\mu$) estimated extinction to be zero (Table 1). However, the presence of many extinct species in the fossil record of auks suggests a failure on the part of our models to detect a phylogenetic signature for extinction. One reason could be the constant rate assumption for extinction in the diversity-dependent models is inadequate, because extinction itself may be diversity-dependent. The constant rates assumption for extinction in our model can be relaxed by allowing both λ and μ to change linearly as a function of increasing diversity. Under this relaxed model, extinction was still estimated to be zero (results not shown). Another possible explanation for the failure of our data to detect extinction is that nested subclades within the auks may have experienced shifts in extinction dynamics. If true, then the phylogenetic signature of extinction may be masked when extinction is estimated for the auk clade as whole. Although shifts in diversification dynamics have been detected in other groups (e.g., Jønsson et al. in press), such rate shift models are likely to be overparameterized for moderately sized datasets such as the auks and we do not test them here.

Perhaps the simplest explanation for the failure of our models to detect a phylogenetic signature of extinction is that extinction was episodic in auks, making it impossible to adequately estimate using current diversity-dependent diversification models. Diversity-dependent diversification models that can directly incorporate fossil species into paleo-diversity estimates through time are needed. The diversity-dependent models of trait evolution we developed here do allow inclusion of fossil species into paleo-diversity estimates. Unfortunately, major gaps in the auk fossil record (only one definitive fossil auk is known prior to the Miocene, and most fossil auks are concentrated in well-studied late-Miocene and Pliocene formations; Becker 1987; Warheit 1992; Mayr 2009, 2011; Wijnker and Olson 2009; Smith 2011; Smith and Clark 2011) precluded us from incorporating fossil species in this study. If diversity-dependent trait evolution has occurred, then including fossil species in paleo-diversity estimates should increase the fit of diversity-dependent models, especially when extinction has been episodic.

Conclusion

Most studies of adaptive radiation utilizing phylogenetic data have either looked for slowdowns in cladogenesis (e.g., Weir 2006; McPeek 2008; Phillimore and Price 2008; Rabosky and Lovette 2008a; Etienne et al. 2012; Jønsson et al. in press) or trait evolution (e.g., Harmon et al. 2010; Mahler et al. 2011) to infer a role of ecological opportunity in driving radiations. Few studies using neontological data have found evidence for slowdowns of both cladogenesis and trait evolution simultaneously (e.g., Slater et al. 2010 and Derryberry et al. 2011 found evidence for the latter but not the former, Kennedy et al. 2012 found evidence for both) as expected under adaptive radiation. Here we find evidence for diversity-dependent slowdowns in both cladogenesis and trait evolution in the auks. We conclude that the radiation of the auks from a gull-like ancestor represents a classic example of adaptive radiation following the evolution of a key innovation (diving ability), which allowed exploitation of a novel resource (fish and plankton deep below the water's surface). We suggest that future studies of adaptive radiation using neontological data should include diversity-dependent models of both cladogenesis and trait evolution, especially where detailed fossil records can aid in the calculation of paleo-diversity levels through time.

ACKNOWLEDGMENTS

We acknowledge previous authors (see Methods) for generating the published sequence dataset for the auks used here. R. Etienne, L. Harmon, J. Kennedy, N. Lovejoy (and lab), A. Phillimore, T. Price, and an anonymous reviewer provided useful comments on the paper. C. Boettiger addressed

questions about the PMC method and R. Etienne provided updated R code for the DDD package. Research was funded by an Natural Sciences and Engineering Research Council of Canada Discovery Grant to JTW.

LITERATURE CITED

Agrawal, A. A., M. Fishbein, R. Halitschke, A. P., Hastings, D. L. Rabosky, and S. Rasmann. 2009. Evidence for adaptive radiation from a phylogenetic study of plant defenses. Proc. Natl. Acad. Sci. USA. 106:18067–18072.

Baker, A. J., S. L. Pereira, and T. A. Paton. 2007. Phylogenetic relationships and divergence times of Charadriiformes genera: multigene evidence for the Cretaceous origin of at least 14 clades of shorebirds. Biol. Lett. 3:205–209.

Becker, J. J. 1987. Neogene avian localities of North America. Smithsonian Institution Press, Washington, DC.

Bédard, J. 1969a. Feeding of the least, crested, and parakeet auklets around St. Lawrence Island, Alaska. Can. J. Zool. 47:1025–1050.

———. 1969b. Adaptive radiation in Alcidae. Ibis. 111:189–198.

———. 1985. Evolution and characteristics of the Atlantic Alcidae. Pp. 1–51 *in* D. N. Nettleship and T. R. Birkhead, eds. The Atlantic alcidae. Academic press, London.

Birt, T. P., H. R. carter, D. L. Whitworth, A. McDonald, and S. H. Newman. 2012. Rangewide population genetic structure of Xantus's Murrelet (*Synthliboramphus hypoleucus*). Auk. 129:44–55.

Blomberg, S. P., T. Garland, and A. R. Ives. 2003. Testing for phylogenetic signal in comparative data: behavioral traits are more labile. Evolution 57:717–745.

Boettiger, C., G. Graham, & P. Ralph. 2012. Is your phylogeny informative? Measuring the power of comparative methods. Evolution 66:2240–2251.

Brown, J. W., and M. V. Van Tuinen. 2011. Evolving perceptions on the antiquity of the modern avian tree. Pp. 306–324 *in* G. Dyke and G. Kaiser, eds. Living dinosaurs: ehe evolutionary history of modern birds. Wiley-Blackwell, West Sussex, UK.

Butler, M. A., and A. A. King. 2004. Phylogenetic comparative analysis: a modeling approach for adaptive evolution. Am. Nat. 164:683–695.

Chandler, R. M., and D. Parmley. 2002. The earliest North American record at auk (Aves: Alcidae) from the late Eocene of central Georgia. Oriole. 68:7–9.

Ciampaglio, C.N., M. Kemp, and D. W. McShea. 2001. Detecting changes in morphospace occupation patterns in the fossil record: characterization and analysis of measures of disparity. Paleobiology 27:695–715.

Coyne, J. A., and H. A. Orr. 2004. Speciation. Sinauer, Sunderland, MA.

Coyne, J. A., and T. D. Price. 2000. Little evidence for sympatric speciation in island birds. Evolution 54:2166–2171.

Derryberry, E. P., S. Claramunt, G. Derryberry, R. T. Chesser, J. Cracraft, A. Alexio, J. Pérez-Emán, J. V. Remsen, Jr., and R. T. Brumfield. 2011. Lineage diversification and morphological evolution in a large-scale continental radiation: the Neotropical ovenbirds and woodcreepers (Aves: Furnariidae). Evolution 65:2973–2986.

Diamond, J. M. 1986. Evolution of ecological segregation in the New guinea montane avifauna. Pp. 98–125 *in* J. M. Diamond and T. J. Case, eds. Community ecology. Harper and Row, New York.

Drummond A. J., and A. Rambaut. 2007. BEAST: Bayesian evolutionary analysis by sampling trees. BMC Evol. Biol. 7:1–8.

Ericson P. G. P., L. Christides, A. Cooper, M. Irestadt, J. Jackson, U. S. Johansson, and J. A. Norman. 2002. A Gondwanan origin of passerine birds supported by DNA sequences of the endemic New Zealand wrens. Proc. R. Soc. Lond. B 269:235–241.

Etienne, R. S., B. Haegeman, T. Stadler, T. Aze, P.N. Pearson, A. Purvis, and A. B. Phillimore. 2012. Diversity-dependence brings molecular phylogenies closer to agreement with the fossil record. Proc. R. Soc. B 279:1300–1309.

Fitzjohn, R. G. 2010. Diversitree: comparative phylogenetic tests of diversification. R package version 0.7-2. Available at http://CRAN.R-project.org.

Freckleton, R. P., and P. H. Harvey. 2006. Detecting non-Brownian trait evolution in adaptive radiations. PLoS Biol. 4:2104–2111.

Friesen, V. L., A. J. Baker, and J. F. Piatt. 1996a. Phylogenetic relationships within the Alcidae (Charadriiformes: Aves) inferred from total molecular evidence. Mol. Biol. Evol. 13:359–367.

Friesen, V. L., W. A. Montevecchi, A. J. Baker, R. T. Barrett, and W. S. Davidson. 1996b. Population differentiation and evolution in the common guillemot (Uria aalge). Mol. Ecol. 5:793–805.

Friesen, V. L., T. P. Birt, J. F. Piatt, R. T. Golightly, S. H. Newman, P. N. Hébert, and G. Gissing. 2005. Population genetic structure in marbled murrelets (*Brachyramphus marmoratus*), and the delineation of 'distinct population segments' for conservation. Cons. Gen. 6: 607–613.

Garland, T., P. H. Harvey, and A. R. Ives. 1992. Procedures for the analysis of comparative data using phylogenetically independent contrasts. Systematic Biology. 41:18–32.

Gaston, A. J., and I. L. Jones. 1998. The auks: alcidae. Oxford Univ. Press, Oxford, UK.

Glor, R. E. 2010. Phylogenetic insights on adaptive radiation. Annu. Rev. Ecol. Ecol. Syst. 41:251–270.

Hackett, S. J., R. T. Kimball, S. Reddy, R. C. K. Bowie, E. L. Braun, M. J. Braun, J. L. Chojnowski, W. A. Cox, K. Han, J. Harshman, et al. 2008. A phylogenomic study of birds reveals their evolutionary history. Science 320:1763–1768.

Hansen, T. F. 1997. Stabilizing selection and the comparative analysis of adaptation. Evolution 51:1341–1351.

Harmon, L. J., J. A. Schulte II, A. Larson, and J. B. Losos. 2003. Tempo and mode of evolutionary radiation in Iguanian lizards. Science 301:961–964.

Harmon, L. J., J. T. Weir, C. D. Brock, R. E. Glor, and W. Challenger. 2008. GEIGER: investigating evolutionary radiations. Bioinformatics 24: 129–131.

Harmon, L. J., J. B. Losos, T. J. Davies, R. G. Gillespie, J. L. Gittleman, W. B. Jennings, K. H. Kozak, M. A. McPeek, F. Moreno-Roark, T. J. Near, et al. 2010. Early bursts of body size and shape evolution are rare in comparative data. Evolution 64:2385–2396.

Irestedt, M, J. Fjeldsa, L. Dalen, and P. G. P. Ericson. 2009. Convergent evolution, habitat shifts and variable diversification rates in the ovenbird-woodcreeper family (Furnariidae). BMC Evol. Biol. 9:1–13.

Johnsen, A., E. Rindal, P. G. P. Ericson, D. Zuccon, K. C. R. Kerr, M. Y. Stoeckle, and J. T. Lifjeld. 2009. DNA barcoding of Scandinavian birds reveals divergent lineages in trans-Atlantic species. J. Ornithol. 151: 565–578.

Jønsson, K. A., P. Fabre, S. A. Fritz, R. S. Etienne, R. E. Ricklefs, T. B. Jørgensen, J. Fjeldså, C. Rahbek, P. G. P. Ericson, F. Woogg, et al. Ecological and evolutionary determinants for the adaptive radiation of the Madagascan vangas. Proc. Natl. Acad. Sci. USA. 109:6620–6625.

Kennedy, J. D., J. T. Weir, D. M. Hooper, D. T. Tietze, J. Martens, and T. D. Price. 2012. Ecological limits on diversification of the Himalayan core Corvoidea. Evolution. 66:2599–2613.

Kidd, M. G., and V. L. Friesen. 1998. Patterns of control region variation in populations of *Cepphus guillemots*: testing microevolutionary hypotheses. Evolution 52:1158–1168.

Kooyman, G. L. 1975. Behaviour and physiology of diving. Pp. 115–137 *in* B. Stonehouse, ed. The biology of penguins. Macmillan Press, Ltd. London.

Kooyman, G. L., R. W. Davies, J. P. Croxall, and D. P. Costa. 1982. Diving depths and energy requirements of King Penguins. Science 217: 726–727.

Losos, J. B. 2010. Adaptive radiation, ecological opportunity, and evolutionary determinism. Am. Nat. 175:623–639.

Mahler, D. L., L. J. Revell, R. E. Glor, and J. B. Losos. 2011. Ecological opportunity and rate of morphological evolution in the diversification of Greater Antillean anoles. Evolution 64:2731–2745.

Mayr, G. 2009. Paleogene fossil birds. Springer, Heidelberg and New York.

———. 2011. The phylogeny of charadriiform birds (shorebirds and allies)—reassessing the conflict between morphology and molecules. Zool. J. Linn. Soc. 161:916–934.

McLoughlin, S. 2001. The breakup history of Gondwana and its impact on pre-Cenozoic floristic provincialism. Aust. J. Bot. 49:271–300

McPeek, M. A. 2008. The ecological dynamics of clade diversification and community assembly. Am. Nat. 172:E270–E284.

Moen, S. M. 1991. Morphologic and genetic variation among breeding colonies of the atlantic puffin (*Fratercula arctica*). Auk. 108:755–763.

Moum, T., U. Arnason, and E. Arnason. 2002. Mitochondrial DNA sequence evolution and phylogeny of the Atlantic Alicidae, including the extinct great auk (*Pinguinus impennis*). Mol. Biol. Evol. 19:1434–1439.

Nee, S., A. O. Mooers, and P. H. Harvey. 1992. The tempo and mode of evolution revealed from molecular phylogenies. PNAS 89:8322–8326.

Nee, S., R. M. May, and P. H. Harvey. 1994. The reconstructed evolutionary process. Phil. Trans. R. Soc. Lond. B 344:305–311.

Nettleship, D. N. 1996. Family Alcidae (Auks). Pp. 679-722 *in* J. del Hoyo, A.Elliott, and J. Sargatal, eds. Handbook of the birds of the world. Vol. 3. Lynx Edicions, Hoatzin to Auks, Barcelona.

Pagel, M. 1994. Detecting correlated evolution on phylogenies: a general method for the comparative analysis of discrete characters. Proc. Roy. Soc. B 255:37–45.

Paton, T. A., and A. J. Baker. 2006. Sequences from 14 mitochondrial genes provide a well-supported phylogeny of the Charadriiform birds congruent with the nuclear RAG-1 tree. Mol. Phylogenet. Evol. 39:657–667.

Paton, T. A., A. J. Baker, J. G. Groth, and G. F. Barrowclough. 2003. RAG-1 seqeunces resolve phylogenetic relationships within Charadriiform birds. Mol. Phylog. Evol. 29:268–278.

Pearce, R. L., J. J. Wood, Y. Artukhin, T. P. Birt, M. Damus, and V. L. Friesen. 2002. Mitochondrial DNA suggests high gene flow in ancient murrelets. Condor 104:84–91.

Pereira, S. L., and A. J. Baker. 2008. DNA evidence for a Paleocene origin of the Alcidae (Aves: Charadriiformes) in the Pacific and multiple dispersals across northern oceans. Mol. Phylo. Evol. 46:430–445.

Phillimore, A. B., and T. D. Price. 2008. Density-dependent cladogenesis in birds. PLoS Biol. 6:483–489.

———. 2009. Ecological influences on the temporal pattern of speciation. Pp. 240–256 *in* J. Bridle Butlin, and D. Schluter, eds. Speciation and patterns of diversity. Cambridge Univ. Press, Cambridge, U.K.

Phillimore, A. B., C. D. L. Orme, G. H. Thomas, T. M. Blackburn, P. M. Bennett, K. J. Gaston, and I. P. F. Owens. 2008. Sympatric speciation in birds is rare: insights from range data and simulations. Am. Nat. 171:646–657.

Piatt, J. F., and D. N. Nettleship. 1985. Diving depths of four alcids. Auk. 102:293-297.

Pigot, A. L., A. B. Phillimore, I. P. F. Owens, and C. D. L. Orme. 2010. The shape and temporal dynamics of phylogenetic trees arising from geographic speciation. Syst. Bio. 59:660-673.

Price, T. D. 2008. Speciation in birds. Roberts and Co, Denver, CO. 480 pp.

Pybus, O. G., and P. H. Harvey. 2000. Testing macro-evolutionary models using incomplete molecular phylogenies. Proc. R. Soc. Lond. B 267:2267–2272.

Rabosky, D. L. 2006. LASER: a maximum likelihood toolkit for detecting temporal shifts in diversification rates from molecular phylogenies. Evol. Bioinform.Online 2:257–260.

Rabosky, D. L., and I. J. Lovette.2008a. Density-dependent diversification in North American wood-warblers. Proc. R. Soc. B 275:2363–2371.

———. 2008b. Explosive evolutionary radiations: decreasing speciation or increasing extinction through time? Evolution 62:1866-1875.

———. 2009. Problems detecting density-dependent diversification on phylogenies: reply to Bokma. Proc. R. Soc. B 276:995–997.

Richman, A. D., and T. D. Price. 1992. Evolution of ecological differences in the Old World leaf warblers (genus *Phylloscopus*): a phylogenetic perspective. Evolution 50:2461–2470.

Schluter, D. 2000. The ecology of adaptive radiation. Oxford Univ. Press, Oxford, UK.

Schorger, A. W. 1947. The deep diving of the loon and old-squaw and its mechanism. Wilson Bull. 59:151–159.

Slater, G. J., S. A. Price, F. Santini, and M. E. Alfaro. 2010. Diversity versus disparity and the radiation of modern cetaceans. Proc. R. Soc. B 277:3097–3104.

Smith, N. A. 2011. Taxonomic revision and phylogenetic analysis of the flightless Mancallinae (Aves, Pan-Alcidae). ZooKeys 91:1–116.

Smith, N. A., and J. A. Clarke. 2011. An alphataxonomic revision of extinct and extant razorbills 9Aves, Alcidae): a combined morphometric and phylogenetic approach. Ornithol. Monogr. 72:1–61.

Vamosi, J. C., and S. M. Vamosi. 2011. Factors influencing diversification in angiosperms: at the crossroads of intrinsic and extrinsic traits. Am. J. Bot. 98:460–471.

Walsh, H. E., and V. L. Friesen. 2003. Patterns of molecular variation at mitochondrial, neutral nuclear, and MHC loci in least and crested auklets (*Aethia* spp.). J. Mol. Evol. 57:681–693.

Warheit, K. I. 1992. A review of the fossil seabirds from the Tertiary of the North Pacific: plate tectonics, paleoceanography, and faunal change. Paleobiology 18:401–424.

Weir, J. T. 2006. Divergent timing and patterns of species accumulation in lowland and highland Neotropical birds. Evolution 60:842–855.

Weir, J. T., and T. Price. 2011. Limits to speciation inferred from times to secondary sympatry along a latitudinal gradient. Am. Nat. 177: 462–469.

Wijnker, E., and S. L. Olson. 2009. A revision of the fossil genus *Miocepphus* and other Miocene Alcidae (Aves: Charadriiformes) of the western North Atlantic Ocean. J. Syst. Paleontol. 7:471–487.

Associate Editor: L. Harmon

Supporting Information

The following supporting information is available for this article:

Figure S1. Time-calibrated phylogeny of auks and outgroups.
Table S1. Genbank accession numbers used.
Table S2. Biogeographic events and fossils used to date nodes.
Table S3. Trait values for auks.

Supporting Information may be found in the online version of this article.

Please note: Wiley-Blackwell is not responsible for the content or functionality of any supporting information supplied by the authors. Any queries (other than missing material) should be directed to the corresponding author for the article.